ACS APPLIED POLYMER MATERIALS

pubs.acs.org/acsapm

Article

Evaluation of Interfacial Shear Strength Healing Efficiency between Dynamic Covalent Bond-Based Epoxy and Functionalized Fiberglass

Federico Benazzo and Henry A. Sodano*

Cite This: ACS Appl. Polym. Mater. 2022, 4, 2925−2934

Read Online

ACCESS | Metrics & More | Article Recommendations | Supporting Information

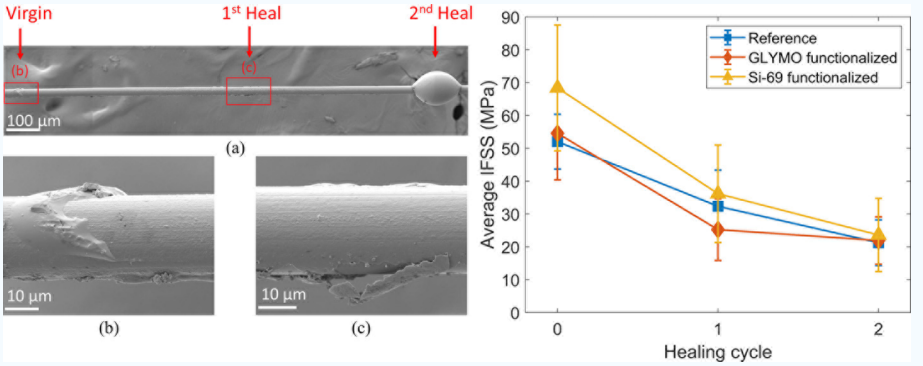

ABSTRACT: Extending the service life of light-weight composite materials used in structural applications has drawn extensive research interests in recent years. One promising solution is the incorporation of self-healing polymers as the matrix component to enable the intrinsic repair of structural damage, thus allowing the composite structure to maintain its mechanical performance and expand its useful life. One of the primary failure mechanisms in composites is interfacial failure, and this research seeks to develop a methodology that enables reformation of covalent crosslinks at the interface to recover material strength. The approach developed here focuses on the evaluation of interfacial shear strength (IFSS) of a composite material system consisting of a self-healing matrix formed by bisphenol-F diglycidyl ether mixed with 4-aminophenyl disulfide (4-AFD) and fiberglass. Interfacial damage is repaired through thermal stimulus that cleaves the dynamic covalent disulfide bonds in the 4-AFD constituent of the matrix followed by bond reformation to return material strength. The extent of interfacial healing was characterized through repeated microdroplet testing and was measured to be 61.7 and 39.7% for once- and twice-healed microdroplets, respectively, thus demonstrating the potential of the chosen composite system to not only exhibit matrix healing, as reported in most studies, on self-healing composites but also at the fiber−matrix interface. The surface chemistry of the glass fibers was modified through silane coupling agents 3-(glycidoxypropyl)trimethoxysilane and bis(triethoxysilylpropyl)tetrasulfide (Si-69) functionalization, and their subsequent effects on the IFSS and healing efficiency of the fiber−matrix system were investigated. The Si-69-functionalized fiberglass exhibited an enhancement in IFSS of 31.5% due to the improved fiber−matrix chemical interactions because of the increase in surface functional group concentrations. Therefore, this work demonstrates the interfacial healing potential of 4-AFD-based polymer matrices when incorporated in glass fiber composites and highlights the promising effects of surface functionalization for simultaneously improving IFSS and maintaining interfacial healing efficiency.

KEYWORDS: *composites, interfacial shear strength, microdroplets, self-healing, intrinsic healing, surface treatments, coupling agents*

1. INTRODUCTION

Fiber−matrix debonding is a common failure mode in composite materials which involves separation of the matrix and reinforcement due to weak interactions between them.[1] In order to circumvent such issues, many research efforts have focused on reinforcing the fiber−matrix interface using various techniques, including but not limited to chemical treatments,[2] whiskerization,[3] and interphase design.[4] However, these techniques typically suffer from one or a number of shortcomings, such as reduced fiber volume fraction, reduced wetting, increased cost, manufacturing complexity, and degradation of the fiber. Additionally, while these methods can reduce the risk of interfacial failure, they are typically rendered ineffective following fiber−matrix debonding as permanent interfacial damage is considered to be irreversible. In contrast, structural damage within the matrix phase has been

Received: February 2, 2022
Accepted: March 3, 2022
Published: March 18, 2022

https://doi.org/10.1021/acsapm.2c00215
ACS Appl. Polym. Mater. 2022, 4, 2925−2934

shown to be repairable through the use of self-healing polymers that are able to maintain their mechanical properties after multiple damage events.[5−7] Such damage repair mechanisms have been shown capable of healing matrix cracking and delamination in composite materials, yet their use to heal fiber−matrix interfacial failure is to be adequately explored.

Self-healing composites are generally classified into two categories depending on their healing mechanism: extrinsic and intrinsic healing.[8] In the case of extrinsic healing, damage repair is achieved using either microcapsules[9−17] or microvessels[18−23] that deliver the healing agent to the site of damage, which then reacts with the matrix phase to repair microcracks. For instance, the works by Toohey et al.,[24] Ghazali et al.,[25] and Trask et al.[26] have proved the effectiveness of these systems in recovering fracture toughness but have also exposed the major limitation of the extrinsic approach, that is, the significant dependence of the healing efficiency on the morphology of the interlaminar damage. Intrinsic healing is achieved in composite materials using a polymer matrix that contains dynamic or reversible crosslinks which can reform across a crack. This can be achieved using a thermoplastic polymer that has shape memory properties such that the material can use diffusion to heal, typically under heat[27−35] or by relying on dynamic bonds within the thermoset polymer molecules that can be broken and reformed through specific chemical reactions.[36−39] Many investigations on thermoplastic polymers have employed poly(ethylene-*co*-methacylic acid) adhesive strips between the central layers of the laminates and presented very high healing efficiencies.[40−43] However, as reported by Wang et al.,[44] the improvement in fracture toughness was matched by a reduction in the shear properties of the laminate. Such challenges can be overcome through the use of thermoset polymers, and one widely studied self-healing polymer is an epoxy resin consisting of bisphenol-A diglycidyl ether (DGEBA) and 4-aminophenyl disulfide (4-AFD), which contains reversible disulfide bonds in the crosslinks formed by the 4-AFD molecules that connect the long polymer chains of DGEBA.

When introduced in large polymeric chains, the disulfide bond in 4-AFD forms an associative covalent adaptive network that provides the basis for self-healing.[38] As presented by Matxain et al.,[45] the healing mechanism is a result of a metathesis reaction between 4-AFD molecules mediated by radicals. More specifically, each reaction involves sulfenyl radicals, consisting of 4-AFD molecules split at the disulfide bond in two symmetrical halves, that are generated during the mechanical fracture of the polymer. Two sulfenyl radicals then approach a full disulfide molecule and attack the sulfur−sulfur bond to form two new disulfide bonds, ultimately converting two disconnected radicals into one new 4-AFD molecule. On its own, the healing reaction occurs at room temperature; however, when introduced in an epoxy, the disulfide reactions are frozen due to the higher glass transition temperature (T_g) of the resin, meaning that the healing is activated via thermal stimulus.[37,46] In addition, this dynamic behavior beyond T_g increases polymer chain movement, which determines a slow decrease in viscosity with increasing temperature, typical of vitrimer materials, and allows for the polymer's recycling both as a neat resin and as a matrix in composite materials.[47] de Luzuriaga et al.[46] did demonstrate that DGEBA/4-AFD matrix composite specimens could recover up to 100% of their original interlaminar shear strength (ILSS) by subjecting specimens to ILSS testing before and after healing cycles. However, the use of multilayered laminates, in which both intralaminar and interlaminar damage can be repaired simultaneously, may have concealed important details about the location and mechanism of the composite's healing process. Thus, despite numerous studies demonstrating the repair of matrix cracking in composite materials through the use of self-healing polymers, it remains unclear if healing takes place at the fiber−matrix interface, within the matrix phase, or both. Given that fiber−matrix debonding is a common failure mode in composites, it is of great importance to enable the healing of interfacial damage such that the mechanical performance can be improved and the cycle life lengthened. Therefore, investigating the fiber−matrix debonding mechanisms and the healing efficiency at the interface is a crucial step to provide further understanding of the potential for self-healing composites. Unfortunately, only a limited understanding of the healing of the fiber−matrix interface can be drawn from the modest number of studies focusing on the interface between healing polymers and nonpolymeric materials. Nonetheless, one study in particular from Xu et al.[48] has presented that a healable coating based on disulfide chemistry could be implemented on the metal surface and maintain its healing efficiency as a thin coating.

The interfacial properties of composite materials are typically characterized using single fibers through microdroplet, pullout, pushout, or segmentation. These methods allow for the quantification of the amount of stress necessary to induce fiber−matrix debonding, known as interfacial shear strength (IFSS), along with the composite's debonding response under continuous loading. Single fiber microdroplet testing was first introduced by Miller et al.,[49] and it involves applying microdroplets of resin to a single filament and subsequent loading of the droplet−fiber interface up until debonding is achieved.[50−56] Microdroplet testing is unique since unlike pushout or pullout, where the fiber is permanently removed from the polymer matrix, or segmentation testing where the fibers suffer tensile failure, microdroplet testing simply induces the sliding of the resin along the fiber. This allows for direct and repeated comparison of interfacial damage and a more accurate assessment of interfacial self-healing efficiency as shown by Peterson et al.[55] In their work, the healing efficiency of the IFSS between a thermosetting resin droplet and a fiber that was previously treated with the same polymer was investigated. Peterson et al. showed that the fiber could be coated with the self-healing polymer and the fiber−matrix bond could be repaired by linking the droplet to the polymer on the fiber surface. The healing efficiency of the droplet was measured as a function of T_g, and it was shown to achieve more than 40% efficiency although a T_g of 30 °C or lower was necessary. This low T_g greatly limits the service temperature and application as a structural material.

In this fiber−matrix, interface healing is studied through microdroplet testing of bisphenol-F diglycidyl ether (DGEBF) and 4-AFD epoxy matrix composites with fiberglass reinforcement. In addition, the effect of surface chemistry on IFSS and healing efficiency is evaluated by employing two different fiber surface functionalization treatments. Finally, greater understanding of the interfacial healing mechanism is obtained using scanning electron microscopy (SEM) imaging of the droplets following failure.

https://doi.org/10.1021/acsapm.2c00215
ACS Appl. Polym. Mater. 2022, 4, 2925−2934

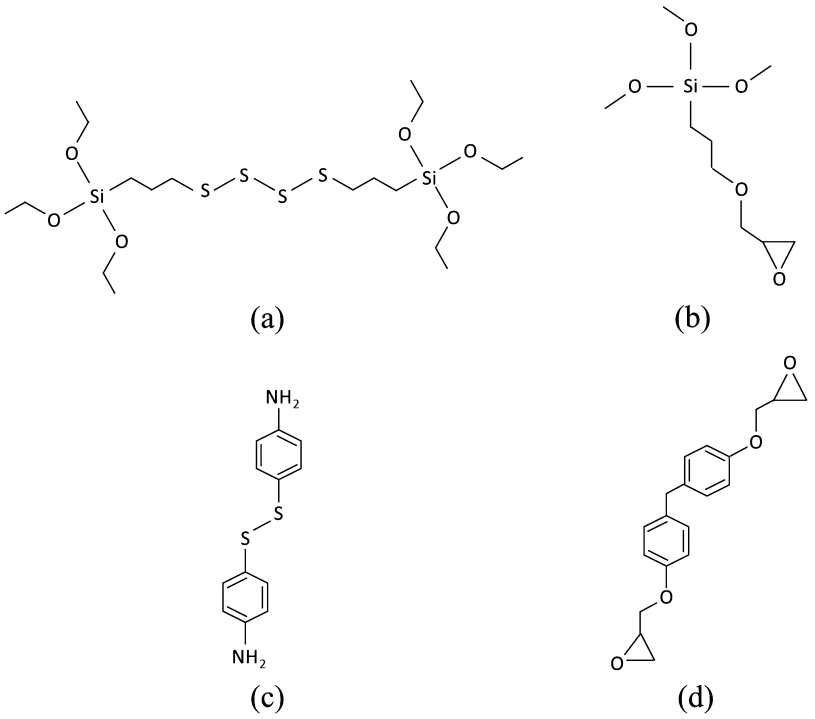

Figure 1. 2D molecular diagrams of (a) Si-69, (b) GLYMO silane coupling agents, (c) 4-AFD, and (d) DGEBF.

2. METHODS

2.1. Materials. Fibers drawn out of an e-glass fabric (Saertex 1200 g/m^2 stitched triaxial fiberglass, FiberGLAST) were subjected to two different surface functionalization treatments in order to evaluate the effect of surface chemistry on IFSS and interfacial healing efficiency. All fibers were cleaned in successive acetone and ethanol baths, followed by drying at 80 °C for 120 min in a vacuum oven. Post cleaning, a set of fiberglass was left untreated, while two other sets of fibers were functionalized using 3-(glycidoxypropyl)trimethoxysilane (GLYMO) and bis(triethoxysilylpropyl)tetrasulfide (Si-69) coupling agents, as shown in Figure 1. The first set of fibers were transferred to a 2 wt % GLYMO volumetric solution of 3:1 ethanol and distilled water that was continuously stirred for 24 h at 120 °C on a heated plate. Concurrently, the second set of fibers were treated in 2 wt % Si-69 dimethyl sulfoxide solution (99.7%, BioReagents, Fisher Scientific) that was heated to 180 °C and continuously stirred for 24 h.

The principal objective of the chosen coupling agents was to assess if surface treatments could improve the measured IFSS without hindering or completely eliminating the polymer's healing efficiency. However, the Si-69 coupling agent was chosen to also evaluate if the sulfur bonds present in the polymer would offer additional sites for the healing of the disulfides in 4-AFD, while GLYMO constituted a set of reference values to compare how the additional sulfur bonds would affect interfacial debonding and healing.

Both functionalized and pristine fibers were laid across Teflon frames (Figure 2) such that microdroplets could be placed in their middle portion. The self-healing resin was prepared as described by Azcune and Odriozola,[37] yet DGEBA was replaced by DGEBF (100%, EPON 862, Hexion) as the choice of prepolymer prior to mixing with 4-AFD (98.0%, TCl America, Fisher Scientific) hardener, as shown in Figure 1. This modification is neither expected to affect the interfacial properties nor the healing mechanism evaluated in this research as both DGEBA and DGEBF exhibit similar functional groups, while the healing mechanism is primarily reliant on the 4-AFD molecule. However, the lower viscosity of DGEBF allows for easier processing and thus improves microdroplet placement on the fiber. To maintain the same ratios of the active hydroxide groups between the prepolymer and the hardener (calculated as 20% more than the stoichiometric ratio) and account for the difference in the molar mass

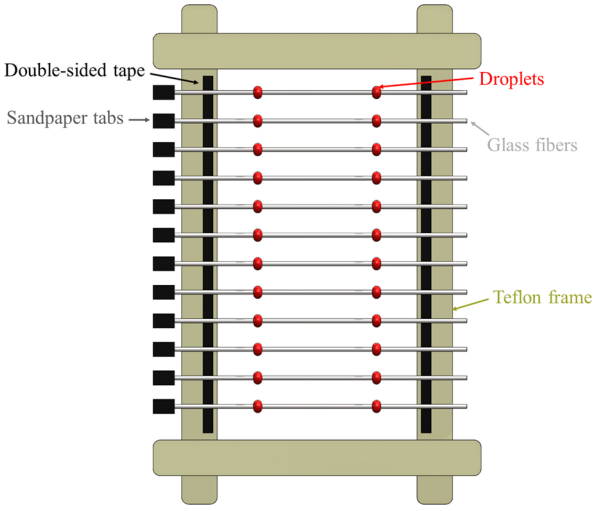

Figure 2. Teflon frame apparatus used for the preparation of microdroplets.

of the two prepolymers, the ratio by weight of the prepolymer to the hardener was changed from 100:42.3 to 100:49.1. After proper mixing, the resin was kept at a temperature of 60 °C, to maintain a low viscosity, and laid on the fibers using tweezers, as suggested by Mcdonough et al.[57] The constant temperature and application methodology, along with optical inspections of the droplets, ensured that only microdroplets with a consistent elliptical shape were tested. These specimens were cured at 120 °C for 120 min and postcured at 150 °C for another 120 min. Finally, sandpaper tabs were attached to one end of the fiber using fast-curing epoxy (EA 9430 adhesive, Loctite) to allow for adequate gripping during interfacial testing. Post testing, interfacial healing was activated by subjecting the microdroplets to a thermal cycle at 200 °C for 10 min.

2.2. Chemical and Optical Characterization of the Materials. Fiberglass surface functionalization was studied through Fourier transform infrared (FTIR) spectroscopy using a Nicolet iS50 spectrometer (Thermo Scientific) with diamond attenuated total

https://doi.org/10.1021/acsapm.2c00215
ACS Appl. Polym. Mater. 2022, 4, 2925−2934

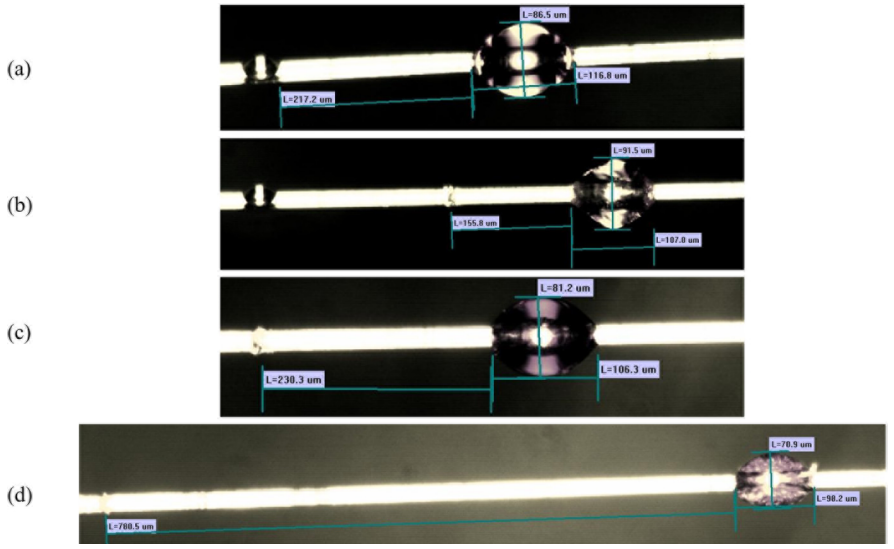

Figure 3. Visual analysis of the mechanical testing and repair of the polymer droplet: (a) Pretesting droplet, (b) post first mechanical test, (c) post second mechanical test, and (d) post third mechanical test (Si-69 fiber). The images show the process used for defining reference points on the fiber related to droplet motion, in addition to the effect of healing cycles [taken place before images (c,d)] on the droplet color.

reflectance. In addition, microdroplet imaging was performed at various steps during the IFSS evaluation process using a Nikon series AZ100 optical microscope. Images of the intact microdroplets were compared to those taken following testing to confirm that failure occurred along the interface as well as for their suitability for healing and subsequent IFSS testing. Optical microscopy was also used to evaluate the length of the droplet–fiber interface which is necessary for IFSS calculations (Figure 3). SEM analysis was carried out on the surface of the tested fibers to qualitatively assess resin distribution on the fiber after droplet interfacial failure. Finally, differential scanning calorimetry (DSC) analysis was performed using a Q2000 calorimeter (TA Instruments) on fragments of polymer droplets to evaluate the epoxy's T_g.

2.3. Microdroplet Test. Microdroplet testing was carried out on a 5982 series Instron load frame equipped with a 5 N load cell according to ASTM standard STP1173.[58] The fibers were gripped at one end using an alligator clip such that the microdroplets were in place between razor blades, as shown in Figure 4. Depending on the

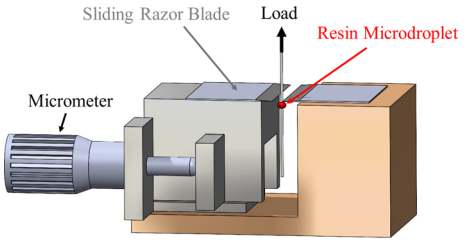

Figure 4. Microdroplet testing device held in place by a screw and bolt that link the apparatus to the Instron frame.

diameter of the microdroplet, the distance between the two razor blades was adjusted using a micrometer to ensure contact. As reported by Eichhorn et al.,[59] this testing approach suffers from a large statistical variation in results, which deems the obtained IFSS values unsuitable for comparisons with other investigation that demonstrate improvements in material properties. However, the objective of this investigation is to compare interfacial properties prior and post healing; therefore, greater emphasis was placed on comparing the % change in IFSS after each healing cycle. In conclusion, the scatter in IFSS is not expected to play such a dominant role in the outcomes of this investigation, even though it must be noted that new difficulties originating from testing the same droplets multiple times do arise.

Inherently to microdroplet testing, load–displacement plots obtained from the experiments may indicate different forms of interfacial mechanisms and failure modes which are further discussed in Supporting Section A. Nonetheless, a maximum load (F_{max}) can generally be identified along with the axial length of the droplet (l) and the diameter of the fiber (d) to calculate the IFSS (τ_s), following eq 1.

$$\tau_s = \frac{F_{max}}{(\pi d)l} \tag{1}$$

As observed in Figure 3 and presented in detail by Miller et al.,[53] the epoxy droplets do not have a perfectly round shape due to the adhesive tension with the fiber. Hence, l was determined to be the distance between the first and last contact points of the droplet–fiber interface. Due to the unavoidable droplet damage during testing, the contact length between the droplet and the fiber was found to change after every test, and therefore, it had to be remeasured prior to retesting. Therefore, the procedure of the experiment consisted in measuring the size of the microdroplets before testing the specimens in the apparatus shown and then healing the same microdroplets through the thermal stimulus. The microdroplets were then subjected to mechanical testing, and finally, the first interfacial healing efficiency was calculated using eq 2 provided by Peterson et al.[55] These steps would then be repeated to determine the second healing efficiency of the microdroplets.

$$\text{Healing efficiency (\%)} = \frac{\text{IFSS}_{\text{repaired}}}{\text{IFSS}_{\text{virgin}}} \times 100 \tag{2}$$

3. RESULTS AND DISCUSSION

3.1. FTIR Analysis. The effect of functionalization treatments on the chemical structure can be assessed using FTIR spectroscopy. As determined in the fiberglass spectra shown in Figure 5a and the corresponding detailed views, multiple peaks corresponding to various functional groups in the coupling agents can be detected. A more detailed analysis of these absorption peaks is presented below and is supported by additional data from previous work reported by Jung et al.[60,61] Compared to the spectrum of the control group, GLYMO- and Si-69-functionalized fibers present three common characteristic peaks that can be attributed to the

https://doi.org/10.1021/acsapm.2c00215
ACS Appl. Polym. Mater. 2022, 4, 2925–2934

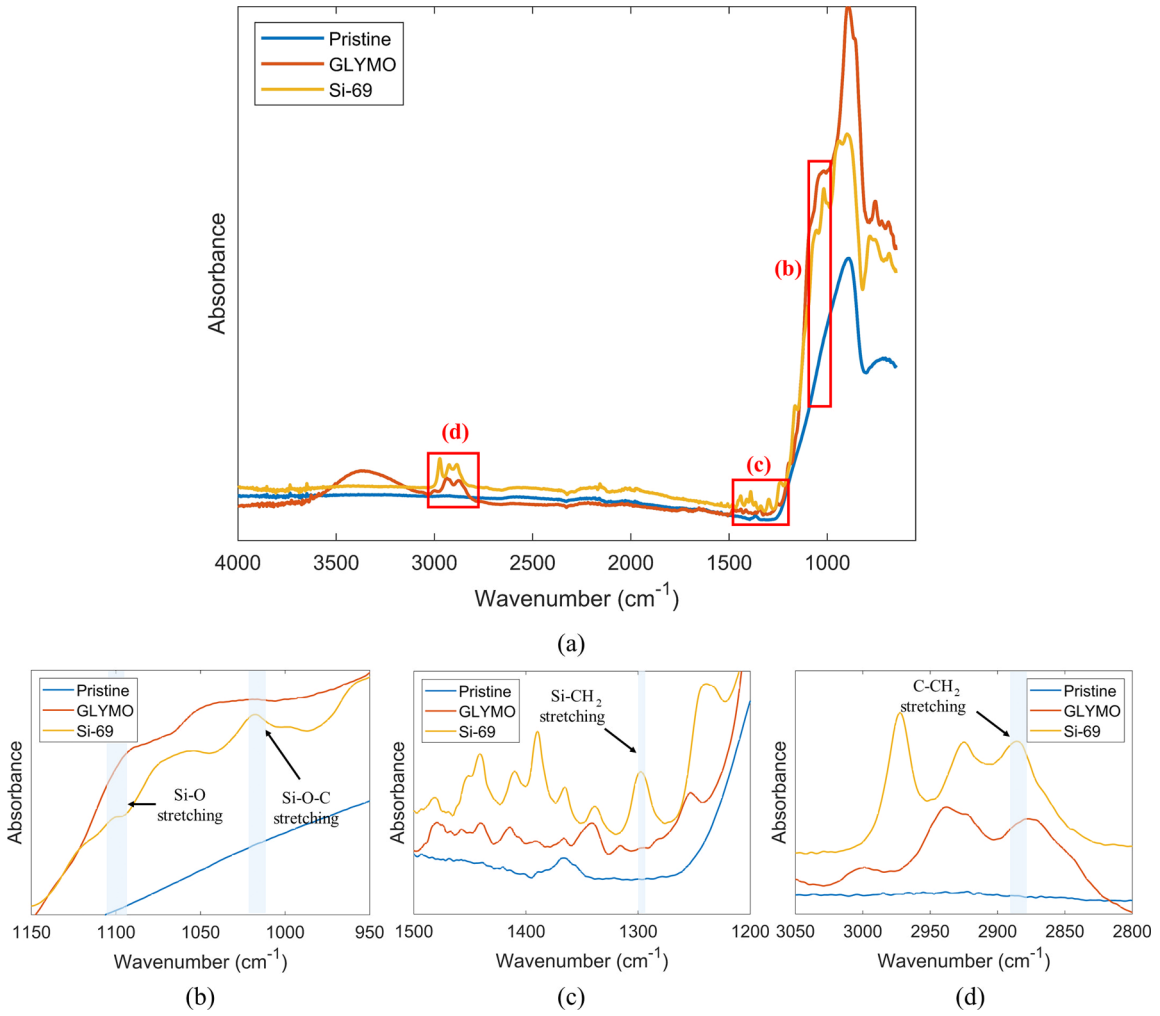

Figure 5. (a) FTIR spectra of pristine fiber and GLYMO-functionalized and Si-69-functionalized fiberglass, along with (b–d) detailed views at various relevant wave number ranges.

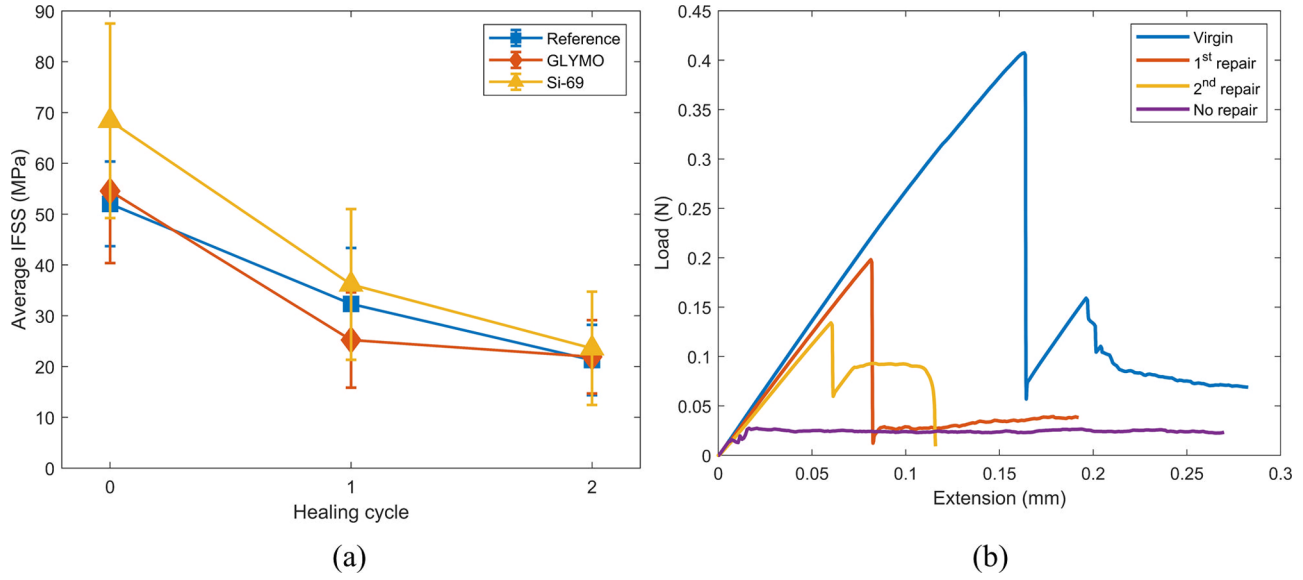

Figure 6. (a) Mean IFSS and corresponding standard deviation for all three sets of single fiberglass reinforced composites and (b) representative load–displacement curve obtained during the microdroplet testing of a single Si-69-functionalized fiberglass specimen, both indicating a decrease in IFSS with successive healing for all fibers.

https://doi.org/10.1021/acsapm.2c00215
ACS Appl. Polym. Mater. 2022, 4, 2925–2934

Table 1. Mean and Standard Deviations of Healing Efficiencies from Figure 8

	average 1st healing eff. (%)	st. dev. 1st healing eff. (%)	average 2nd healing eff. (%)	st. dev. 2nd healing eff. (%)	# samples for 2nd healing
reference	61.7	17.4	39.6	9.8	8
GLYMO	47.2	16.1	39.7	7.2	5
Si-69	54.3	21.4	31.7	10.3	11

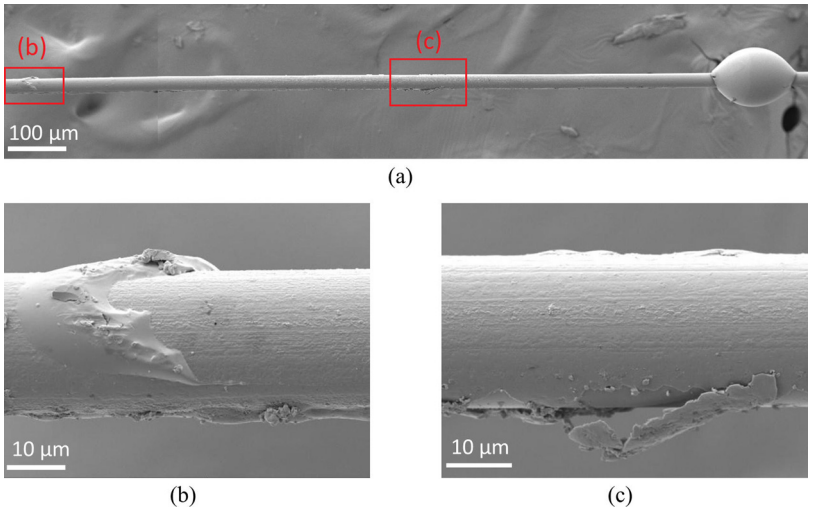

Figure 7. SEM images of a GLYMO fiber and its microdroplet with detailed views of the fractured portions of the droplet. Image (a) presents the whole fiber surface along with the microdroplet, while (b,c) are close-ups of the two anchor points where the droplet originally formed the fiber−matrix interface. The resin in (b) represents the anchor point that was established during the curing process and fractured during the first mechanical test, while that in (c) represents the anchor point formed during the healing process and fractured during the second mechanical test.

coupling agents: the stretching of Si−O−C and Si−O at 1017 and 1100 cm^{-1} and the stretching of methylene groups at 2875 cm^{-1}. The presence of these additional functional groups determines a higher concentration of reactive sites to which the epoxy polymer chains may react during the curing process. Additionally, Si-69-functionalized fibers display a peak at 1300 cm^{-1} that is attributed to the stretching of S−CH_2 (Figure 5c), which is unique to this coupling agent. Therefore, identification of the characteristic absorption peaks of the coupling agents on fiberglass surface through FTIR analysis confirms successful fiber functionalization processes.

3.2. Discussion of Interfacial Healing Performance. The results of microdroplet testing data clearly indicate that a portion of the IFSS is found to be restored, implying that the fiber−matrix interface heals after being exposed to a thermal cycle. The direct comparison of the load−displacement curves (Figure 6b) of the healed and nonrepaired polymer droplets demonstrate that the healed interface requires a significant load to break the reformed fiber−matrix bond, while the droplet that was not subjected to the healing cycle slides freely when a load greater than the interfacial friction is applied. As observed in Figure 6a and Table 1, a maximum interfacial healing efficiency of 61.7% was measured when using reference fiberglass after the first damage event, outperforming the GLYMO and Si-69 fiberglass by 14.5 and 7.4% respectively. Healing of the fiber−matrix interface can be reasoned to be due to epoxy's relaxation at high temperatures. Once exposed to temperatures greater than its T_g of 129 °C, as measured using DSC analysis (Figure S3), the resin matrix is expected to relax and expand, causing a compressive stress on the fiber and filling any inherent microscopic gaps and grooves present on the fiber surface. Once cooled down, the dynamic disulfide bonds reform the crosslinks in the epoxy resin, thus reducing the molecule chains mobility and "freezing" the matrix in a compressive sheathe around the fiber. These newly formed anchoring sites can be detected through SEM imaging in the form of small, fractured portions of the droplets that remain attached to the fiber surface. The remaining matrix residues shown in Figure 7b,c is a sign of cohesive failure and constitute further evidence of a strong fiber−matrix interface both prior and post healing. In addition, the SEM images display a fiber surface that is not perfectly smooth, with microscale trenches, thus supporting the explanation of the matrix relaxation in the fiber's grooves. The high degree of healing ability of the fiber−matrix interface is to be attributed in part to considerations of the stress relaxation of the 4-AFD based matrix presented in the material characterization by de Luzuriaga et al.[46] In their thermal evaluation, stress relaxation curves at 200 °C presented extremely rapid relaxation in the range of tens of seconds, that, when compared to other resins with the same prepolymer,[62] clearly indicate the considerably faster thermal relaxation of the 4-AFD based resin. This rapid change in viscosity of the resin, along with the compression from the thermal expansion of the resin, suggests that the matrix was able to adhere to the microscopic trenches in the glass fiber and form new interfacial bonds. The bonding in this posthealing fiber−matrix interface is different from the chemical bonding created during the curing process, in that it is more a mechanical link based on frictional forces. Yet, it provides a resistance to shear comparable to that of the virgin samples.

Following the second fiber−matrix debonding event, a smaller, yet considerable, fraction of IFSS is found to be recoverable, as only a maximum interfacial healing of 39.7% is achieved. The observed decrease in healing efficiencies can be attributed to the change in droplet shape after their first mechanical test and healing cycles. As observed in Figure 3,

https://doi.org/10.1021/acsapm.2c00215
ACS Appl. Polym. Mater. 2022, 4, 2925−2934

microdroplet testing causes the droplets to experience substantial damage at their lateral extremities where the droplet comes in contact with the edges of the razor blades. Such damage is unavoidable, as microdroplet extremities have been shown to be weak points and high stress concentration zones.[52] This causes the flattening of the contact area between the droplet and the blade, transitioning the microdroplet from an elliptical to a cylindrical shape. Previous work has numerically and empirically shown that IFSS measurements when using a spherical microdroplet are significantly smaller than their elliptical counterparts.[52] Additionally, while the length of the droplets was remeasured after each test, it remains difficult to correctly assess the new length of the interface post healing as only the outer surface of the droplet is visible under a microscope or SEM. Thus, the obtained measurements represent an upper bound of the contact length, which may be considerably shorter if portions of the droplets have been lost during mechanical testing, resulting in underestimation regarding IFSS and healing efficiency. It should be noted that the number of samples tested after second healing is considerably smaller than earlier rounds of testing and is found to vary between data sets. This is attributed to the fragile nature of microdroplets, which causes the majority of droplets to suffer critical fracture, making them unsuitable for further testing after the first healing and testing processes. Despite these difficulties, it can be concluded that the healing mechanism of the interface is different from that inferred for matrix cracking repair by de Luzuriaga et al.,[46] and fiber−matrix debonding can be repaired with this resin.

3.3. Healing with Fiber Functionalization. When comparing the IFSS of Si-69- and GLYMO-functionalized fibers relative to those of reference ones (Figure 6), considerable improvement in interfacial properties is observed for Si-69 treated fibers, irrespective of the healing cycle. Specifically, as presented in Table 2, virgin, once-healed, and twice-healed Si-69-functionalized fibers were found to exhibit 31.5, 11.9, and 10.9% increase in IFSS relative to the reference fiber at similar healing cycles, respectively. Increments in IFSS after fiber functionalization have been shown in various works[2,63,64] and can be directly attributed to the increase in fiber surface reactivity. The functional groups introduced by the coupling agents improve the chemical interaction between the fiber and the resin, enhancing fiber−matrix bonding and increasing IFSS. Additionally, the superior performance of Si-69 functionalization relative to the GLYMO one can be attributed to its larger number of functional groups, which provide a higher concentration of bonding sites for the resin and yield better adhesion between the fiber and the matrix, thus reducing slipping during mechanical loading.

Table 2. Percentage Changes in IFSS with Respect to the Reference Fibers

	GLYMO (%)	Si-69 (%)
increment of IFSS in virgin samples	4.8	31.5
increment of IFSS in once-healed samples	−22.0	11.9
increment of IFSS in twice-healed samples	3.0	10.9

A comparison of the healing efficiencies (Figure 8) shows that the functionalized fibers presented similar, if not slightly underperforming results with respect to the reference fibers, with a maximum reduction of 14.5% in once-healed GLYMO-treated fibers. The same GLYMO samples later showed an average healing efficiency 0.1% higher than the reference samples, which illustrates the inconsistency in the extent of healing of the fiber−matrix interface, caused by the experimental difficulties inherent to microdroplet testing presented in the previous section. In general, it can still be inferred that treating the fiber with silane coupling agents will not eliminate the healing ability of the fiber−matrix combination, and fiber functionalization is a suitable method to improve IFSS without greatly affecting the healing efficiency. Nonetheless, the functionalization through Si-69 did not appear to promote the formation of dynamic disulfide bonds between the fiber and the matrix since there was no improvement in the healing efficiency of the droplets. This is most likely caused by the far too different molecular structures around the coupling agent's and the resin's sulfur bonds that do not allow the bonding between sulfurs from the two polymeric structures after cleavage. Future studies may involve treating the fibers with various other coupling agents to assess their compromise between IFSS and healing efficiency.

4. CONCLUSIONS AND FUTURE IMPROVEMENTS

The results presented in this work demonstrate that the healing properties of the DGEBF mixed with 4-AFD epoxy resin can be exploited to repair the fiber−matrix interface of composite materials through a healing mechanism based on the matrix relaxation at T_g and the fiberglass' surface imperfections. As shown through microdroplet testing, the IFSS of once- and twice-healed specimens can be restored to a maximum average of 61.7 and 39.7%, respectively, through mechanical rebonding of the fiber−matrix interface. Additionally, it was determined that Si-69-functionalized fibers presented maximum improvements of 31.5, 11.9, and 10.9% in the virgin, once-healed, and twice-healed IFSS, respectively, with minor influences on the measured healing efficiencies, thus proving that enhancements to interfacial bonding can be obtained while sustaining the healing efficiency ability of the fiber−matrix interface. Nonetheless, the introduced sulfur bonds on the Si-69-functionalized fiber surface were determined to yield no improvement in the interfacial healing efficiency due to the absence of reformed disulfide bonds between Si-69 and the matrix. In conclusion, these results deepen the understanding and application of this healing resin, which was limited to evaluations of matrix microcracking, and demonstrate the polymer's ability to repair fiber−matrix debonding—therefore improving the performance of composite materials and reducing their failure risks.

Future works could involve a series of approaches to improve the composite's IFSS while maintaining the healing efficiency. Since the composite system consists of a common e-glass fiber and a less common resin, it is still categorized as a thermosetting epoxy. Several surface treatments that have been shown to improve IFSS in similar composites, which include filling multiwall carbon nanotubes in the interfacial region,[65] grafting zinc oxide nanowires on the surface of the fiber,[66] and doping the matrix phase with polystyrene nanofibers to improve adhesion to the fibers,[67] could be employed. Improving the interfacial healing efficiency is instead a more challenging task due to the little research that has been performed on the subject. Most of the studies on healing matrices focus on the repair of interlaminar mechanical properties, such as delamination, and thus do not offer inspiration on how to enhance the restoring ability of the matrix with regards to IFSS. However, it was shown by

https://doi.org/10.1021/acsapm.2c00215
ACS Appl. Polym. Mater. 2022, 4, 2925−2934

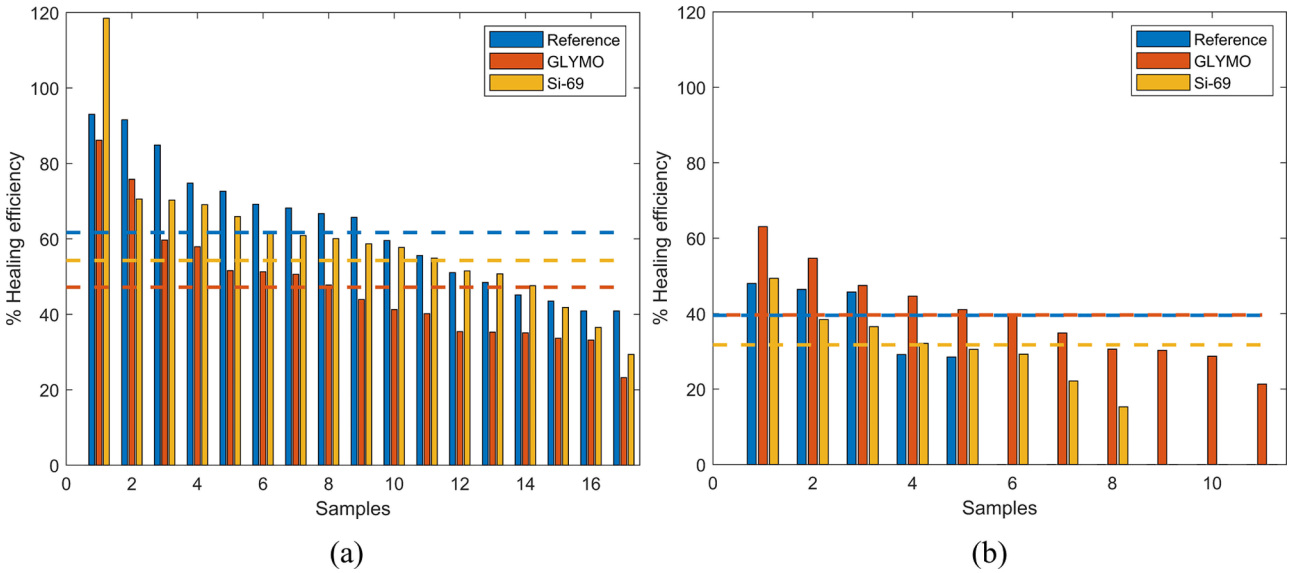

Figure 8. (a) First and (b) second healing efficiency of the polymer microdroplet−fiber interface, ordered from the largest to smallest efficiency, with a dashed line representing the average for each set of fibers.

Peterson et al.[55] that previously coating the fibers with the thermoplastic matrix later employed to manufacture the microdroplets offered a high healing efficiency at the expense of the service temperature of the composite. Thus, the fiber treatment with the 4-AFD based epoxy resin is an approach that could be employed in the future to attempt further improvement of the IFSS healing efficiency.

■ ASSOCIATED CONTENT

Supporting Information

The Supporting Information is available free of charge at https://pubs.acs.org/doi/10.1021/acsapm.2c00215.

Representative load−displacement plots of different microdroplet tests and representative microscope image of the damaged droplet; DSC data of the DGEBF and 4-AFD based polymer; and table clearly listing the values presented in Figure 6 (PDF)

■ AUTHOR INFORMATION

Corresponding Author

Henry A. Sodano − *Department of Aerospace Engineering, Department of Materials Science and Engineering, and Department of Macromolecular Science and Engineering, University of Michigan, Ann Arbor 48109 Michigan, United States;* orcid.org/0000-0001-6269-1802; Email: hsodano@umich.edu

Author

Federico Benazzo − *Department of Aerospace Engineering, University of Michigan, Ann Arbor 48109 Michigan, United States;* orcid.org/0000-0001-6307-5737

Complete contact information is available at: https://pubs.acs.org/10.1021/acsapm.2c00215

Notes

The authors declare no competing financial interest.

■ ACKNOWLEDGMENTS

The authors gratefully acknowledge support for this work from the National Science Foundation under grant # CMMI-1762369 and the Air Force Office of Scientific Research under contract # FA9550-21-1-0019.

■ REFERENCES

(1) Callister, W.; Rethwish, D. Failure. In *Materials Science and Engineering: An Introduction*, 10th ed.; Wiley, 2018; Chapter 8.

(2) Brodowsky, H. M.; Hennig, A.; Müller, M. T.; Werner, A.; Zhandarov, S.; Gohs, U. Laccase-Enzyme Treated Flax Fibre for Use in Natural Fibre Epoxy Composites. *Materials* **2020**, *13*, 4529.

(3) Majumdar, A.; Singh Butola, B.; Awasthi, N.; Chauhan, I.; Hatua, P. Improving the Mechanical Properties of P-Aramid Fabrics and Composites by Developing ZnO Nanostructures. *Polym. Compos.* **2018**, *39*, 3300−3306.

(4) Nasser, J.; Steinke, K.; Zhang, L.; Sodano, H. Enhanced Interfacial Strength of Hierarchical Fiberglass Composites through an Aramid Nanofiber Interphase. *Compos. Sci. Technol.* **2020**, *192*, 108109.

(5) Kostopoulos, V.; Kotrotsos, A.; Tsokanas, P.; Tsantzalis, S. Toughening and Healing of Composites by CNTs Reinforced Copolymer Nylon Micro-Particles. *Mater. Res. Express* **2018**, *5*, 025305.

(6) Hart, K. R.; Wetzel, E. D.; Sottos, N. R.; White, S. R. Repeatable Self-Healing of an Epoxy Matrix Using Latent 2-Ethyl-4-Methyl-imidazole Catalyst. In *29th Annual Technical Conference of the American Society for Composites, ASC 2014; 16th US-Japan Conference on Composite Materials; ASTM-D30 Meeting*, 2014.

(7) Cohades, A.; Michaud, V. Thermal Mending in E-Glass Reinforced Poly(ε-Caprolactone)/Epoxy Blends. *Composites, Part A* **2017**, *99*, 129−138.

(8) Meure, S.; Wu, D. Y. The Biomimetic Approach to Self Healing Polymer Composite Development in the Aerospace Industry. In *Proceedings of the First International Conference on Self-Healing Materials*; Springer, 2007.

(9) Brown, E. N.; Sottos, N. R.; White, S. R. Fracture Testing of a Self-Healing Polymer Composite. *Exp. Mech.* **2002**, *42*, 372−379.

(10) Chowdhury, R. A.; Hosur, M. V.; Nuruddin, M.; Tcherbi-Narteh, A.; Kumar, A.; Boddu, V.; Jeelani, S. Self-Healing Epoxy Composites: Preparation, Characterization and Healing Performance. *J. Mater. Res. Technol.* **2015**, *4*, 33−43.

(11) Ghazali, H.; Ye, L.; Zhang, M. Q. Interlaminar Fracture of CF/EP Composite Containing a Dual-Component Microencapsulated Self-Healant. *Composites, Part A* **2016**, *82*, 226−234.
(12) Kessler, M. R.; White, S. R. Self-Activated Healing of Delamination Damage in Woven Composites. *Composites, Part A* **2001**, *32*, 683−699.
(13) Manfredi, E.; Cohades, A.; Richard, I.; Michaud, V. Assessment of Solvent Capsule-Based Healing for Woven E-Glass Fibre-Reinforced Polymers. *Smart Mater. Struct.* **2014**, *24*, 015019.
(14) Patel, A. J.; Sottos, N. R.; Wetzel, E. D.; White, S. R. Autonomic Healing of Low-Velocity Impact Damage in Fiber-Reinforced Composites. *Composites, Part A* **2010**, *41*, 360−368.
(15) Tripathi, M.; Rahamtullah; Kumar, D.; Rajagopal, C.; Kumar Roy, P. Influence of Microcapsule Shell Material on the Mechanical Behavior of Epoxy Composites for Self-healing Applications. *J. Appl. Polym. Sci.* **2014**, *131*, 40572.
(16) White, S. R.; Sottos, N. R.; Geubelle, P. H.; Moore, J. S.; Kessler, M. R.; Sriram, S. R.; Brown, E. N.; Viswanathan, S. Autonomic Healing of Polymer Composites. *Nature* **2001**, *409*, 794−797.
(17) Yin, T.; Zhou, L.; Rong, M. Z.; Zhang, M. Q. Self-Healing Woven Glass Fabric/Epoxy Composites with the Healant Consisting of Micro-Encapsulated Epoxy and Latent Curing Agent. *Smart Mater. Struct.* **2007**, *17*, 015019.
(18) Bekas, D. G.; Baltzis, D.; Paipetis, A. S. Nano-Reinforced Polymeric Healing Agents for Vascular Self-Repairing Composites. *Mater. Des.* **2017**, *116*, 538−544.
(19) Aniskevich, A.; Vidinejevs, S.; Kulakov, V.; Strekalova, O. Development of Composites with a Self-Healing Function. *Mater. Des.* **2015**, *21*, 32−37.
(20) Norris, C. J.; Bond, I. P.; Trask, R. S. Interactions between Propagating Cracks and Bioinspired Self-Healing Vascules Embedded in Glass Fibre Reinforced Composites. *Compos. Sci. Technol.* **2011**, *71*, 847−853.
(21) Norris, C. J.; Bond, I. P.; Trask, R. S. Healing of Low-Velocity Impact Damage in Vascularised Composites. *Composites, Part A* **2013**, *44*, 78−85.
(22) Saeed, M. U.; Li, B. B.; Chen, Z. F.; Cui, S. Self-Healing of Low-Velocity Impact and Mode-I Delamination Damage in Polymer Composites via Microchannels. *eXPRESS Polym. Lett.* **2016**, *10*, 337−348.
(23) Kato, Y.; Minakuchi, S.; Ogihara, S.; Takeda, N. Self-Healing Composites Structure Using Multiple through-Thickness Microvascular Channels. *Adv. Compos. Mater.* **2020**, *30*, 1−18.
(24) Toohey, K. S.; Sottos, N. R.; Lewis, J. A.; Moore, J. S.; White, S. R. Self-Healing Materials with Microvascular Networks. *Nat. Mater.* **2007**, *6*, 581−585.
(25) Ghazali, H.; Ye, L.; Zhang, M. Q. Mode II Interlaminar Fracture Toughness of CF/EP Composite Containing Microencapsulated Healing Resins. *Compos. Sci. Technol.* **2017**, *142*, 275−285.
(26) Trask, R. S.; Norris, C. J.; Bond, I. P. Stimuli-Triggered Self-Healing Functionality in Advanced Fibre-Reinforced Composites. *J. Intell. Mater. Syst. Struct.* **2014**, *25*, 87−97.
(27) Buitrago, C. F.; Pressly, J. F.; Yang, A. S.; Gordon, P. A.; Riggleman, R. A.; Natarajan, B.; Winey, K. I. Creep Attenuation in Glassy Polymer Nanocomposites with Variable Polymer−Nanoparticle Interactions. *Soft Matter* **2020**, *16*, 8912−8924.
(28) Ipakchi, H.; Rezadoust, A. M.; Esfandeh, M.; Rezaei, M. An Investigation on the Effect of Polyvinyl Butyral Interlayer Forms on the Fracture Toughness of Glass Reinforced Phenolic Laminates. *Thin-Walled Struct.* **2020**, *151*, 106724.
(29) Jony, B.; Mulani, S. B.; Roy, S. Mode II Fracture Toughness Recovery of CFRP Composite Using Thermoplastic Shape Memory Polymer Healant. In *AIAA Scitech 2020 Forum; AIAA SciTech Forum*; American Institute of Aeronautics and Astronautics, 2020.
(30) Jony, B.; Roy, S.; Mulani, S. B. Fracture Resistance of In-Situ Healed CFRP Composite Using Thermoplastic Healants. *Mater. Today Commun.* **2020**, *24*, 101067.
(31) Jony, B.; Thapa, M.; Mulani, S. B.; Roy, S. Repeatable Self-Healing of Thermosetting Fiber Reinforced Polymer Composites with Thermoplastic Healant. *Smart Mater. Struct.* **2019**, *28*, 025037.
(32) Kotrotsos, A.; Kostopoulos, V. 18—Self-Healing of Structural Composites Containing Common Thermoplastics Enabled or Not by Nanotechnology as Healing Agent. In *Self-Healing Composite Materials*; Khan, A., Jawaid, M., Raveendran, S. N., Ahmed Asiri, A. M., Eds.; Woodhead Publishing Series in Composites Science and Engineering; Woodhead Publishing, 2020; pp 327−374.
(33) Meure, S.; Wu, D. Y.; Furman, S. Polyethylene-Co-Methacrylic Acid Healing Agents for Mendable Epoxy Resins. *Acta Mater.* **2009**, *57*, 4312−4320.
(34) Narducci, F.; Lee, K.-Y.; Pinho, S. T. Interface Micro-Texturing for Interlaminar Toughness Tailoring: A Film-Casting Technique. *Compos. Sci. Technol.* **2018**, *156*, 203−214.
(35) Thapa, M.; Jony, B.; Mulani, S. B.; Roy, S. Experimental Characterization of Shape Memory Polymer Enhanced Thermoplastic Self-Healing Carbon/Epoxy Composites. In *AIAA Scitech 2019 Forum; AIAA SciTech Forum*; American Institute of Aeronautics and Astronautics, 2019.
(36) Aguirre De Cárcer, I.; Prolongo, M. G.; Salom, C.; Parrado, J.; Moriche, R.; Prolongo, S. G. Thermal and Mechanical Properties of Self-Healing Epoxy/Graphene Nanocomposites. In *VIII ECCOMAS Thematic Conference on Smart Structures and Materials*, 2017; pp 1399−1408.
(37) Azcune, I.; Odriozola, I. Aromatic Disulfide Crosslinks in Polymer Systems: Self-Healing, Reprocessability, Recyclability and More. *Eur. Polym. J.* **2016**, *84*, 147−160.
(38) Grande, A. M.; Martin, R.; Odriozola, I.; van der Zwaag, S.; Garcia, S. J. Effect of the Polymer Structure on the Viscoelastic and Interfacial Healing Behaviour of Poly(Urea-Urethane) Networks Containing Aromatic Disulphides. *Eur. Polym. J.* **2017**, *97*, 120−128.
(39) Park, J. S.; Darlington, T.; Starr, A. F.; Takahashi, K.; Riendeau, J.; Thomas Hahn, H. Multiple Healing Effect of Thermally Activated Self-Healing Composites Based on Diels−Alder Reaction. *Compos. Sci. Technol.* **2010**, *70*, 2154−2159.
(40) Ladani, R. B.; Pingkarawat, K.; Nguyen, A. T. T.; Wang, C. H.; Mouritz, A. P. Delamination Toughening and Healing Performance of Woven Composites with Hybrid Z-Fibre Reinforcement. *Composites, Part A* **2018**, *110*, 258−267.
(41) Pingkarawat, K.; Wang, C. H.; Varley, R. J.; Mouritz, A. P. Self-Healing of Delamination Cracks in Mendable Epoxy Matrix Laminates Using Poly[Ethylene-Co-(Methacrylic Acid)] Thermoplastic. *Composites, Part A* **2012**, *43*, 1301−1307.
(42) Shanmugam, L.; Naebe, M.; Kim, J.; Varley, R. J.; Yang, J. Recovery of Mode I Self-Healing Interlaminar Fracture Toughness of Fiber Metal Laminate by Modified Double Cantilever Beam Test. *Compos. Commun.* **2019**, *16*, 25−29.
(43) Varley, R. J.; Parn, G. P. Thermally Activated Healing in a Mendable Resin Using a Non Woven EMAA Fabric. *Compos. Sci. Technol.* **2012**, *72*, 453−460.
(44) Wang, C. H.; Sidhu, K.; Yang, T.; Zhang, J.; Shanks, R. Interlayer Self-Healing and Toughening of Carbon Fibre/Epoxy Composites Using Copolymer Films. *Composites, Part A* **2012**, *43*, 512−518.
(45) Matxain, J. M.; Asua, J. M.; Ruipérez, F. Design of New Disulfide-Based Organic Compounds for the Improvement of Self-Healing Materials. *Phys. Chem. Chem. Phys.* **2016**, *18*, 1758−1770.
(46) de Luzuriaga, A. R.; Martin, R.; Markaide, N.; Rekondo, A.; Cabañero, G.; Rodríguez, J.; Odriozola, I. Epoxy Resin with Exchangeable Disulfide Crosslinks to Obtain Reprocessable, Repairable and Recyclable Fiber-Reinforced Thermoset Composites. *Mater. Horiz.* **2016**, *3*, 241−247.
(47) Paolillo, S.; Bose, R. K.; Santana, M. H.; Grande, A. M. Intrinsic Self-Healing Epoxies in Polymer Matrix Composites (PMCs) for Aerospace Applications. *Polymers* **2021**, *13*, 201.
(48) Xu, H.; Tu, J.; Xiang, G.; Zhang, Y.; Guo, X. A Thermosetting Polyurethane with Excellent Self-Healing Properties and Stability for Metal Surface Coating. *Macromol. Chem. Phys.* **2020**, *221*, 2000273.

(49) Miller, B.; Muri, P.; Rebenfeld, L. A Microbond Method for Determination of the Shear Strength of a Fiber/Resin Interface. *Compos. Sci. Technol.* **1987**, *28*, 17−32.
(50) An, F.; Lu, C.; Li, Y.; Guo, J.; Lu, X.; Lu, H.; He, S.; Yang, Y. Preparation and Characterization of Carbon Nanotube-Hybridized Carbon Fiber to Reinforce Epoxy Composite. *Mater. Des.* **2012**, *33*, 197−202.
(51) Gaur, U.; Miller, B. Microbond Method for Determination of the Shear Strength of a Fiber/Resin Interface: Evaluation of Experimental Parameters. *Compos. Sci. Technol.* **1989**, *34*, 35−51.
(52) Kang, S.; Lee, D.; Choi, N. Fiber/Epoxy Interfacial Shear Strength Measured by the Microdroplet Test. *Compos. Sci. Technol.* **2009**, *69*, 245−251.
(53) Miller, B.; Gaur, U.; Hirt, D. E. Measurement and Mechanical Aspects of the Microbond Pull-out Technique for Obtaining Fiber/Resin Interfacial Shear Strength. *Compos. Sci. Technol.* **1991**, *42*, 207−219.
(54) Park, J.-M.; Wang, Z.-J.; Kwon, D.-J.; Gu, G.-Y.; Um, M.-K.; DeVries, K. L. Evaluation of Interfacial Properties and Microfailure Mechanisms in Single Fiber-Reinforced Epoxy Composites at Low Temperature. *Polym. Compos.* **2012**, *33*, 147−157.
(55) Peterson, A. M.; Jensen, R. E.; Palmese, G. R. Kinetic Considerations for Strength Recovery at the Fiber-Matrix Interface Based on the Diels-Alder Reaction. *ACS Appl. Mater. Interfaces* **2013**, *5*, 815−821.
(56) Peterson, A. M.; Jensen, R. E.; Palmese, G. R. Thermoreversible and Remendable Glass−Polymer Interface for Fiber-Reinforced Composites. *Compos. Sci. Technol.* **2011**, *71*, 586−592.
(57) McDonough, W. G.; Antonucci, J. M.; Dunkers, J. P. Interfacial Shear Strengths of Dental Resin-Glass Fibers by the Microbond Test. *Dent. Mater.* **2001**, *17*, 492−498.
(58) Leadbetter, K.; Latour, R.; Johnson, R.; Shalaby, S. *Micromechanical Testing of Interfacial Bonding in Absorbable Composites*; ASTM International, 1994.
(59) Eichhorn, S. J.; Bennett, J. A.; Shyng, Y. T.; Young, R. J.; Davies, R. J. Analysis of Interfacial Micromechanics in Microdroplet Model Composites Using Synchrotron Microfocus X-Ray Diffraction. *Compos. Sci. Technol.* **2006**, *66*, 2197−2205.
(60) Jung, J.; Sodano, H. A. Aramid Nanofiber Reinforced Rubber Compounds for the Application of Tire Tread with High Abrasion Resistance and Fuel Saving Efficiency. *ACS Appl. Polym. Mater.* **2020**, *2*, 4874−4884.
(61) Jung, J.; Sodano, H. A. High Strength Epoxy Nanocomposites Reinforced by Epoxy Functionalized Aramid Nanofibers. *Polymer* **2020**, *195*, 122438.
(62) Tangthana-umrung, K.; Poutrel, Q. A.; Gresil, M. Epoxy Homopolymerization as a Tool to Tune the Thermo-Mechanical Properties and Fracture Toughness of Vitrimers. *Macromolecules* **2021**, *54*, 8393−8406.
(63) Park, J. M.; Subramanian, R. V. Interfacial Shear Strength and Durability Improvement by Monomeric and Polymeric Silanes in Basalt Fiber/Epoxy Single-Filament Composite Specimens. *J. Adhes. Sci. Technol.* **1991**, *5*, 459−477.
(64) Wu, Q.; Wan, Q.; Yang, X.; Wang, F.; Bai, H.; Zhu, J. Remarkably Improved Interfacial Adhesion of Pitch-Based Carbon Fiber Composites by Constructing a Synergistic Hybrid Network at Interphase. *Compos. Sci. Technol.* **2021**, *205*, 108648.
(65) Wang, Z.; Yang, B.; Xian, G.; Tian, Z.; Weng, J.; Zhang, F.; Yuan, S.; Ding, X. An Effective Method to Improve the Interfacial Shear Strength in GF/CF Reinforced Epoxy Composites Characterized by Fiber Pull-out Test. *Compos. Commun.* **2020**, *19*, 168−172.
(66) Steinke, K.; Sodano, H. A. Enhanced Interfacial Shear Strength in Ultra-High Molecular Weight Polyethylene Epoxy Composites through a Zinc Oxide Nanowire Interphase. *Compos. Sci. Technol.* **2022**, *219*, 109218.
(67) Nguyen, D. D.; Vu, C. M.; Choi, H. J. Improvement of the Mode I Interlaminar Fracture Toughness of Glass Fiber/Epoxy Composites Using Polystyrene Electrospun Nanofibres. *Polym. Bull.* **2018**, *75*, 5089−5102.

https://doi.org/10.1021/acsapm.2c00215
ACS Appl. Polym. Mater. 2022, 4, 2925−2934